



PAPER • OPEN ACCESS

Global drought risk in cities: present and future urban hotspots

To cite this article: Tristian R Stolte *et al* 2023 *Environ. Res. Commun.* **5** 115008

View the [article online](#) for updates and enhancements.

You may also like

- [Dynamic risk assessment method of urban drought based on water balance and optimal allocation analysis](#)
Keke Sun, Jijun Xu, Liqiang Yao et al.
- [Multi-scale planning model for robust urban drought response](#)
Marta Zaniolo, Sarah Fletcher and Meagan S Mauter
- [Trans-boundary variations of urban drought vulnerability and its impact on water resource management in Singapore and Johor, Malaysia](#)
C Joon Chuah, Beatrice H Ho and Winston T L Chow

Environmental Research Communications



PAPER

Global drought risk in cities: present and future urban hotspots

OPEN ACCESS

RECEIVED
21 February 2023

REVISED
9 June 2023

ACCEPTED FOR PUBLICATION
10 October 2023

PUBLISHED
14 November 2023

Original content from this work may be used under the terms of the [Creative Commons Attribution 4.0 licence](#).

Any further distribution of this work must maintain attribution to the author(s) and the title of the work, journal citation and DOI.



Tristian R Stolte¹ , Hans de Moel¹ , Elco E Koks¹ , Marthe L K Wens¹ , Felix van Veldhoven² , Snigdha Garg³, Neuni Farhad³ and Philip J Ward¹

¹ Institute for Environmental Studies, Vrije Universiteit Amsterdam, Amsterdam, the Netherlands

² Climate Adaptation Services, Bussum, the Netherlands

³ C40 Cities, NY, United States of America

E-mail: Tristian.stolte@vu.nl

Keywords: urban drought risk, hydrological drought, global disaster risk, urban agglomerations, disaster risk management, drought hotspots, urban disaster risk

Supplementary material for this article is available [online](#)

Abstract

Hydrological droughts pose a persistent threat for cities and are increasingly studied. However, this is rarely within a large-scale context, complicating comparisons between cities and potentially hampering the most efficient allocation of resources in terms of drought risk adaptation and mitigation. Here, we investigate global urban hydrological drought risk for 264 urban agglomerations across all continents for both the present time and future projections. To derive risk profiles for each agglomeration, we include components of: drought hazard (drought volume focusing on surface water deficits), exposure (urban population), vulnerability (multivariate vulnerability index), and cost (replacement of freshwater expenses). These components are dynamic in time, except for vulnerability. Most agglomerations are projected to experience an increase in drought hazard, exposure, and cost by 2050, with the most notable current and future hotspot being northern South Asia (India & Pakistan). Also, the number of agglomerations with high risk increases, whereas the number with lower risk decreases, indicating that high urban drought risk is increasing in scale over time. Our results enable a better targeting of those agglomerations that need most urgent attention in terms of drought risk solutions. It can also be used to identify agglomerations with similar drought risk profiles that could be studied in conjunction and may benefit from cooperative drought risk management strategies.

1. Introduction

Droughts are enigmatic in character (Mishra and Singh 2010), but despite their fuzziness, we can define the essence of drought as a temporal deficiency of water at any stage in the hydrological cycle (e.g. lack of rain or discharge) relative to the average climatic situation of the area where it occurs (Van Loon and Van Lanen 2013, Van Loon 2015, WMO and GWP 2016). Although often associated with agricultural areas, droughts are also an urban challenge (Singh *et al* 2021). In the past, several cities have experienced adverse impacts from droughts. For example, Mexico City (2010), São Paulo (2015) and Cape Town (2015–2017) have all experienced severe reductions in public water supply from (multi-year) droughts (Simpkins 2018). Past events like those show that droughts affect cities either: (i) directly, by reducing public water or hydropower energy supplies, or (ii) indirectly, for instance by increasing food prices; causing or aggravating poverty, supply-chain interruptions, health issues, and social instability; and reducing water quality and industrial productivity (Grant *et al* 2013, Hsiang *et al* 2013, Stanke *et al* 2013, Nobre *et al* 2016, Von Uexkull *et al* 2016, Van Lanen *et al* 2017, Desbureaux and Rodella 2019, Zhang *et al* 2019, Ziervogel 2019, UNDRR 2021). For instance, during the Cape Town drought, reservoir levels dropped to only 20% of their capacity and urban residents had to reduce their water consumption by up to 50% (Simpkins 2018, Ziervogel 2019). In Beijing, insufficient rain caused a deficit between water demand and water supply of around 10 billion m³ per year (Wang *et al* 2017). Current estimates suggest

that droughts will occur more frequently and/or with higher intensity in many regions around the globe due to climate change (Arias *et al* 2021, UNDRR 2021), which could lead to a further aggravation of urban drought impacts.

Droughts, like other natural hazards, pose a continuous threat to society, which is often referred to as disaster risk. The risk is defined as the function of: (i) a hazardous event; (ii) the exposed elements to such an event; and (iii) the vulnerability of those exposed elements to the hazard (UNDRR 2019). Disaster risk models are used to assess spatial patterns and temporal trends in risk in order to inform policy and decision makers on present and future disaster risk (Ward *et al* 2020). At the global scale, several drought risk assessments have been performed by applying such models, but most do not explicitly consider cities or omit them completely. Instead, their focus has often been on agricultural practices (e.g. Yin *et al* 2014, Guo *et al* 2016, Arnell *et al* 2018, Meza *et al* 2020, Haqiqi *et al* 2021), a set of specific economic sectors (e.g. Stahl *et al* 2016, Naumann *et al* 2021), or people and income in general (i.e. population and GDP, e.g. Liu and Chen 2021, Carrão *et al* 2016, Winsemius *et al* 2018).

Although urban drought risk studies at the continental to global scale are not entirely absent (Güneralp *et al* 2015, Guerreiro *et al* 2018), they often use simplified measures of hazard and exposure and generally lack a vulnerability component. For instance, Güneralp *et al* (2015) only look at the number of urban expansion located in drylands, without considering actual water supply/demand or vulnerability for those urban regions. Guerreiro *et al* (2018) do model the water supply, but do not account for the actual location of urban water sources, nor do they incorporate vulnerability. The lack of risk components in these studies is not surprising, as urban drought is a relatively new field and information on urban drought risk is scarce (Singh *et al* 2021), which impedes comprehensive assessments of urban drought risk. Instead, global urban studies about water shortage have focused primarily on water scarcity (McDonald *et al* 2014, Flörke *et al* 2018, He *et al* 2021). Although water scarcity and droughts can result in similar socioeconomic impacts, their nature is different, as water scarcity refers to water shortage over the long term or as a system state (i.e. decades and longer), whereas droughts have a temporary nature (i.e. days to several years; Van Loon 2015). Hence, cities that are not water scarce can still be impacted by droughts (UNDRR 2021). Moreover, droughts can also aggravate water shortage in water scarce regions and may cause additional impacts (UNDRR 2021). So we argue that a global urban drought assessment is of added benefit to the existing global urban water scarcity studies.

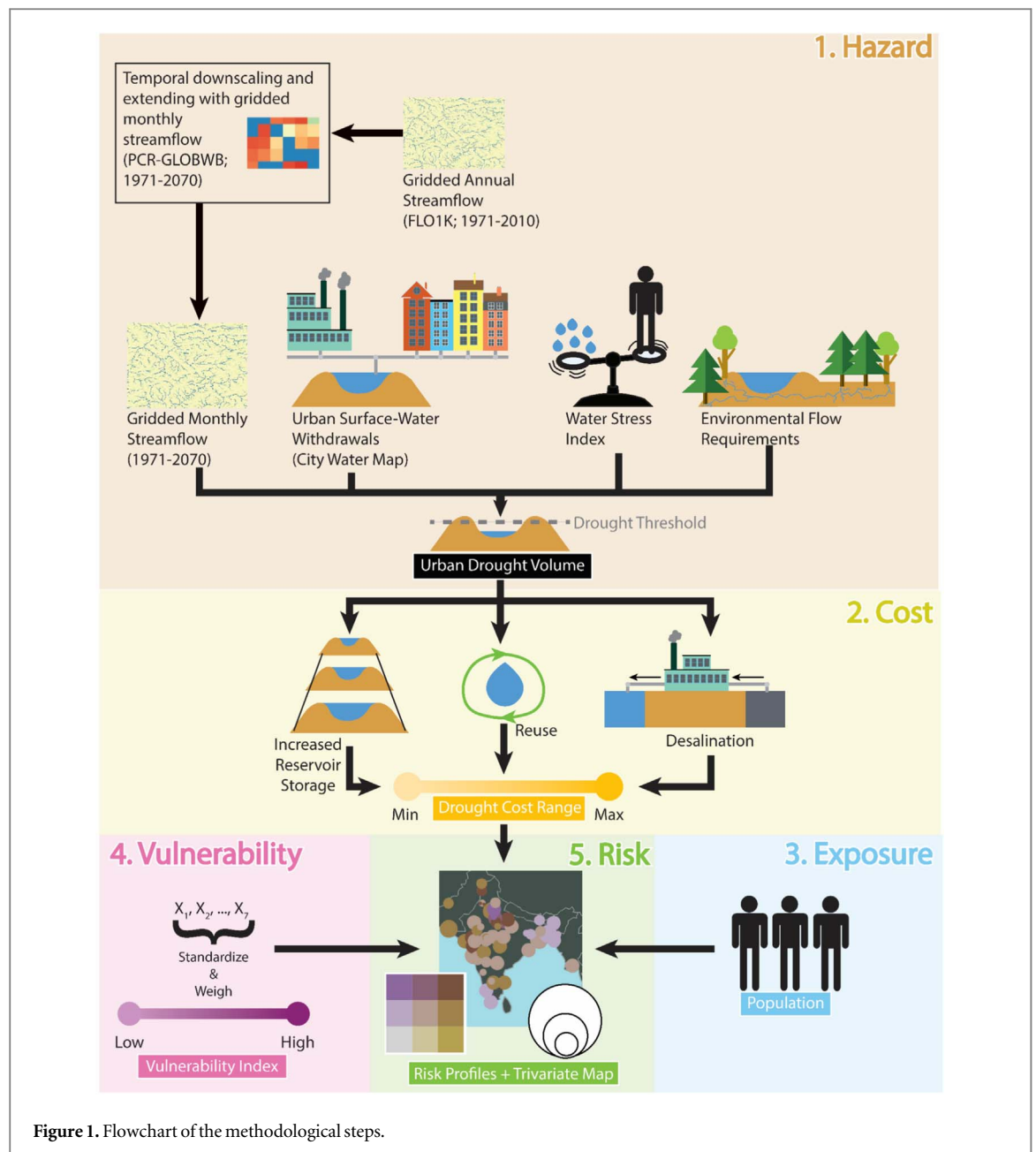
As cities play an increasingly important role in dealing with global challenges, such as reducing disaster risk and the impacts of climate change (UN 2017, Rosenzweig *et al* 2010), more urban-focused drought risk research is essential to provide cities with the necessary information. Cities are also concentrated pools of exposed elements to natural hazards including droughts (Pesaresi *et al* 2017, Gu 2019). Whilst cities cover only 2%-3% of the Earth's surface (Liu *et al* 2014), they are inhabited by over half of the world's population, and this is projected to increase to two-thirds by 2050. Moreover, roughly 80% of the global GDP is generated in cities (UN-Habitat 2018). Nevertheless, regardless of the importance of cities in dealing with global challenges, drought has so far received little attention in urban policy making (Cremades *et al* 2021, Singh *et al* 2021). Most urban data and knowledge are currently unevenly distributed over regions and institutions (McPhearson *et al* 2016, Acuto *et al* 2018), which makes it challenging to assess global patterns of urban drought risk and to compare the risk between different cities. A global-scale urban drought risk assessment is required to aid policy makers, city practitioners, and other urban-focused institutes to identify cities with the most urgent need for improved drought risk management or to even put drought risk on the agenda of cities in the first place.

Our study aims to provide this global overview of urban drought risk by carrying out a global-scale analysis for 264 urban agglomerations. The goal is to find global patterns of drought risk as well as the underlying patterns of drought hazard, exposure, and vulnerability. We will focus on hydrological droughts, which relates to deficits of streamflow and groundwater (Dracup *et al* 1980, Van Loon *et al* 2016), because the impacts of drought on cities are mostly originating from either of these water sources. We will focus specifically on surface water deficits, because groundwater modeling generally has more uncertainty than streamflow modeling (De Graaf *et al* 2015, Tangdamrongsub *et al* 2017). For the assessment, we develop an open-source framework to identify hazard, exposure, and vulnerability indicators, and to provide a qualitative risk estimate. We perform the assessment under both historical and future (2050) climate conditions, using a variety of climate and socio-economic scenarios.

2. Methods

2.1. Overview

The flowchart in figure 1 provides a general overview of the five steps taken in this study, which relate to simulating and assessing: (i) drought hazard; (ii) drought costs; (iii) exposure; (iv) vulnerability; and (v) risk, following the risk framework of Kron (2005), and the IPCC (2014). We focus on 264 urban agglomerations



distributed globally, based on data availability (section 2.4). Each urban agglomeration has one or multiple surface water source locations from which it extracts its municipal water requirements for consumptive and economic use (McDonald *et al* 2014, 2016). We assume that an agglomeration enters hydrological drought conditions as soon as the water level at its source locations drops below a certain threshold. Thus, urban hydrological drought, hereafter referred to as urban drought, is here defined as the water that an agglomeration requires but which it cannot extract from its surface-water source locations due to climatologically drier conditions than normal.

In step 1, to represent the hazard, we evaluate the drought volume for each agglomeration (section 2.2). We use the City Water Map V2.2 (CWM; McDonald *et al* 2014, 2016) to derive the volume of urban surface water withdrawals (i.e. the freshwater that is extracted at the source locations) (section 2.2.1). To derive the drought threshold, we determine the variation in monthly streamflow at each source location (section 2.2.2), along with the Water Stress Index (2.2.3) and the Environmental Flow Requirements (section 2.2.4). Using this threshold, we can calculate the annual drought volume for each agglomeration (section 2.2.5). At step 2, to end up with a more impact-based risk metric, we multiply the drought volumes with the replacement costs of freshwater to create a proxy for urban drought costs, following several freshwater gaining measures of which unit costs are available globally (increased reservoir storage, reuse, and desalination; section 2.3). Next, in step 3 we derive the exposure by delineating each agglomeration and deriving its total population (section 2.4). For step 4, we gather several vulnerability indicators and combine them into one index to add qualitative information on the

agglomerations (section 2.5). Lastly, in step 5, all these components are combined into a risk metric (section 2.6). The analysis is carried out for the time period 1971–2010 to derive the present situation. To assess the impact of climate change and population growth, we perform the same analysis for the period 2031–2070, using two combinations of Representative Concentration Pathways (RCPs) and Shared Socioeconomic Pathways (SSPs): SSP1+RCP2.6 and SSP3+RCP6.0.

We took care to match the time periods of the different input data as much as possible, but not all data is available for exactly the same historical and future time periods and some data may only partially overlap. One of these data is the Water Stress Index, for which we argue that the difference in time (i.e. the average around 2014 for the Water Stress Index VS 1971–2010 for the other hazard data) is sufficiently small to enable comparison of the data, since the WSI is only mutating significantly over decadal or longer time scales (Huang *et al* 2021). Furthermore, we use cost data from different years, based on the most recent open source information available (Straatsma *et al* 2020), and converted to 2005USD to enable comparison. Lastly, the indicators that we use to compose the vulnerability index are from different sources and we use the most recent values for each city to get the best estimate of the current state of a city's vulnerability

2.2. Drought hazard

2.2.1. Urban surface water withdrawals

To determine a drought threshold for each agglomeration, we first need to assess their surface-water use. The CWM provides a comprehensive overview of water-source locations for 534 urban agglomerations, including surface-water withdrawal information for 291 agglomerations. This information is either based on annual reports from the water utilities that serve the agglomeration or extracted from the websites of those water utilities (McDonald *et al* 2016). Furthermore, McDonald *et al* (2014), (2016) connected each water-source location to the outlet of its reservoir so that the streamflow at those locations represents the situation in the reservoir. Since the water-use information is static and does not include information on inter- or intra-annual variability and since there is no global information at city-level on how water use evolves over time, we set the drought volume proportional to the streamflow below a threshold; for a given extraction point, a 20% drop in streamflow below the threshold equals a 20% drop in extractions. In addition, we consider human and natural water use when creating this threshold, the reason being that cities have to deal with competing water users, such as agriculture (Flörke *et al* 2018), and vegetation and animals (Pastor *et al* 2014).

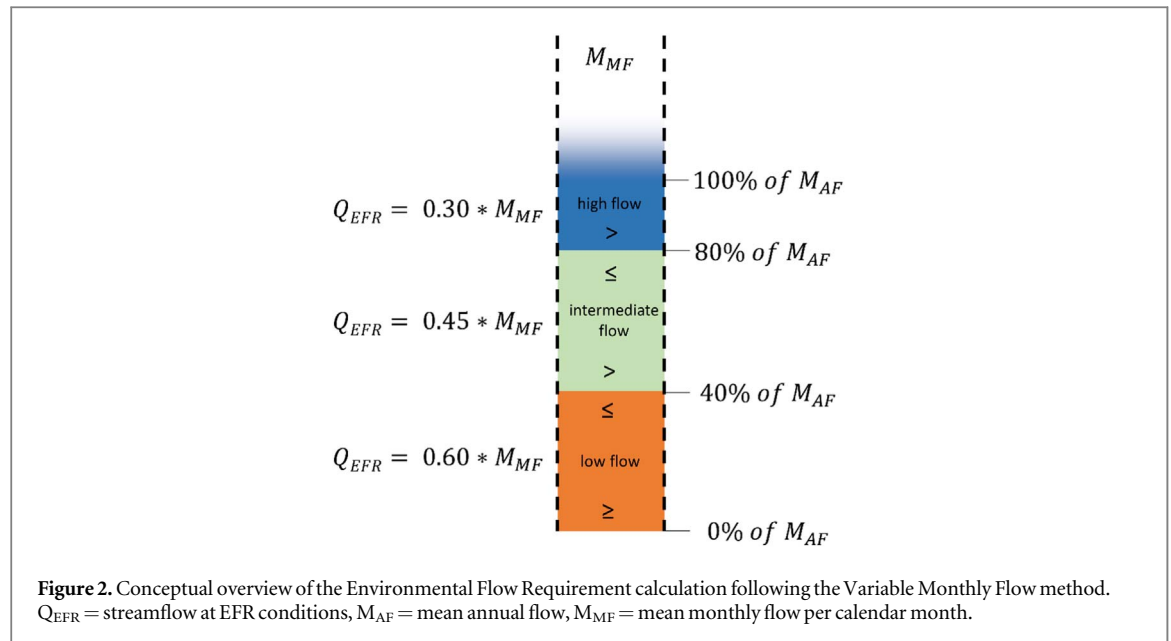
2.2.2. Water supply (gridded monthly streamflow)

For each source location, the water use needs to be compared against the water supply in order to derive a drought threshold. Water supply is defined as the total available streamflow. For this research, we require a streamflow dataset that is: (i) naturalized, because we want to account for human and natural water needs, which are taken relative to the normal hydrological situation; (ii) preferably at a relatively high resolution, since the withdrawal locations are precisely defined; and (iii) based on observations, since we know the absolute extraction volumes of each agglomeration, whereas modeled streamflow data can have a systematic bias in absolute volumes (Zaherpour *et al* 2018). Considering these criteria, a suitable dataset would be the global 30 arcseconds gridded average streamflow data from FLO1K (Barbarossa *et al* 2018). Note that FLO1K's streamflow is 'semi natural': on the one hand, FLO1K is the result of a neural network based on 6,600 observation stations that are not all in natural catchments, while, on the other hand, the authors still describe it as '... the discharge that would occur if there were a natural watercourse.' (Barbarossa *et al* 2018).

FLO1K only provides annual streamflow data, so it cannot capture inter-annual drought variability, yet hydrological conditions can vary strongly within a year (see e.g. Van Loon and Van Lanen 2012). We therefore resample FLO1K to a monthly timestep using streamflow data from the PCRaster GLOBal Water Balance model, PCR-GLOBWB. We use the PCR-GLOBWB streamflow data that were forced with observed climate data at the resolution of 0.5° and at a daily timestep from the WATCH Forcing Data methodology applied to ERA-Interim (WFDEI, Weedon *et al* 2014) data from the Inter-Sectoral Impact Model Intercomparison Project 2a (ISIMIP2a) simulation round (Sutanudjaja *et al* 2018). To resample FLO1K, we take the PCR-GLOBWB streamflow and calculate the relative difference of each monthly mean against the annual mean for each year in the historical time period (1971–2010). Subsequently, we apply those differences to the FLO1K annual mean for that year, to derive FLO1K streamflow with monthly timesteps (equation (1)).

$$Q_{\text{FLO1K},m,y,c} = \frac{Q_{\text{pia},m,y,c}}{Q_{\text{pia},y,c}} * Q_{\text{FLO1K},y,c} \quad (1)$$

Where: Q_{FLO1K} = streamflow from FLO1K; Q_{pia} = streamflow from PCR-GLOBWB forced with ISIMIP2a-WFDEI; m = calendar month; y = year; and c = grid cell. Note that $Q_{\text{pia},y,c}$ and $Q_{\text{FLO1K},y,c}$ denote the average streamflow over all months in year y .



2.2.3. Water stress index

Hydrological drought impacts are more likely to occur in highly water-stressed watersheds, i.e. watersheds with a high use-to-availability ratio, as there is less buffer against a drop in streamflow. We therefore adjust the drought threshold to the urban-focused Water Stress Index (WSI), following He *et al* (2021); equation (2):

$$W_{WSI,b} = \frac{W_{W,b}}{W_{A,b}} \quad (2)$$

Where: $W_{WSI,b}$ = the WSI in river basin b (basins defined by Masutomi *et al* 2009); W_W = total water withdrawals of the combined irrigation, industrial, and residential sectors; W_A = total water availability in the form of runoff.

This index ranges between 0 (i.e. large quantities of water are available for use) and 1 (i.e. all the water in a watershed has been allocated to anthropogenic uses). Furthermore, He *et al* (2021) made the index urban specific by accounting for the in- and outflow of water for the urban agglomerations in each catchment, as defined by the CWM (McDonald *et al* 2014, 2016).

Future total water availability from He *et al* (2021) does not follow the same climate scenarios as those for the other input data that we use. Hence, we derive the total water availability from daily 0.5° runoff data from PCR-GLOBWB from the ISIMIP2b simulation round. For the historical time period, this means that we take the average value within a 20-year time window centered around the target year 2014 (2004-2023), which is the year for which the total withdrawals are known. This methodology results in twelve WSI-values, one for each calendar month, in the historical time period. For the future time period, see 2.2.6.

2.2.4. Environmental flow requirements

To account for natural water use, and to prevent overestimating water availability to the city (Gerten *et al* 2013), we incorporate the Environmental Flow Requirements (EFR), which is defined as the volume of water that is required to maintain the freshwater ecology in a watershed. EFR is often expressed as a fraction of the average streamflow in a watershed (Pastor *et al* 2014). A large EFR means that a larger portion of the streamflow goes to ecological maintenance, which entails a higher hydrological drought threshold for a given watershed, and thus larger droughts compared to watersheds with a lower EFR.

The EFR differs strongly in time and space (Poff and Zimmerman 2010, Pastor *et al* 2014), and requires large amounts of input data to model. Therefore, global EFR estimates are generally based on a single threshold, but these do not account for intra-annual differences because of data constraints. As a midway solution, we apply the Variable Monthly Flow (VMF; Pastor *et al* 2014) method, which requires only the mean annual and monthly naturalized streamflow to calculate intra-annually varying EFR values. It distinguishes between low flow, intermediate flow, and high flow seasons, and for each flow season, another formula is applied to determine the EFR (Pastor *et al* 2014; figure 2). For example: if the mean monthly flow (M_{MF}) is lower than 40% of the mean annual flow (M_{AF}), there is a low flow season, and the Q_{EFR} is set at 60% of the M_{MF} . Both M_{AF} and M_{MF} are based on the FLO1K-resampled streamflow and are taken over the historical time period (1971-2010). The VMF method results in twelve Q_{EFR} values, one per calendar month, for each surface-water source location.

2.2.5. Present drought volumes

To find the present drought hazard, all input data are used to calculate the annual average drought volume per agglomeration over the historical period 1971–2010. For each agglomeration, surface-water source locations are identified, and the corresponding Q_{FLO1K} , W_{WSI} , and Q_{EFR} values are collected in order to calculate a drought threshold per calendar month (equation (3)).

$$Q_{thres,m,s} = \bar{Q}_{FLO1K,m,s}^{1971-2010} * (W_{WSI,m,s} + Q_{EFR,m,s}) \quad (3)$$

Where: $Q_{thres,m,s}$ = streamflow threshold below which drought occurs per calendar month (m) and surface-water source location (s).

In the next step, for each source location, the resampled monthly time series of streamflow is compared against these thresholds. If the streamflow for any given month drops below the threshold, drought conditions occur, and the magnitude of the drought is expressed as the percentage of the water that is missing, relative to the streamflow under normal climatic conditions (equation (4)).

$$V_{perc,m,y,s} = \frac{\max(Q_{thres,m,s} - Q_{FLO1K,m,y,s}, 0)}{\bar{Q}_{FLO1K,m,s}^{1971-2010}} \quad (4)$$

Where V_{perc} is the relative drought volume.

The absolute drought volume of an agglomeration is determined by multiplying the relative drought volume with the water withdrawal volume of that agglomeration at the source location. If an agglomeration has multiple source locations, then the drought volumes are accumulated into one value. The drought volume per month is subsequently aggregated in annual values for the historical time period, and averaged again to obtain one annual average drought volume per agglomeration.

2.2.6. Climate change and future drought volumes

To assess the effect of climate change on hydrological drought in urban areas, we perform the same analysis for a future time period between 2031–2070. We consider two future climate scenarios, using combinations of Representative Concentration Pathways (RCPs) and Shared Socioeconomic Pathways (SSPs): SSP1+RCP2.6, which is the low emission pathway with sustainable development; and SSP3+RCP6.0, which relates to a regional rivalry pathway with a more national-oriented focus and under medium-high emissions (O'Neill *et al* 2014). The data that we use does not allow for other RCP and SSP combinations, but we are confident that these scenarios cover a sufficiently large range of possible drought risk futures. Note that the RCP scenarios refer to possible future states of the climate, and that the SSPs refer to possible future socioeconomic trends (Riahi *et al* 2017). We therefore use the RCP scenarios to simulate future hazard, the SSP scenarios to simulate future exposure, and the combined scenarios to simulate future risk.

To maintain a consistent climatic baseline, the thresholds for both the historical as well as the future time periods make use of the same mean streamflow per calendar month ($\bar{Q}_{FLO1K,m,s}^{1971-2010}$), and the same corresponding EFRs ($Q_{EFR,m,s}$). However, the WSI does change with time, to represent changes in socioeconomic development. In practice, this means that future hazard conditions could be affected by either a change in: (i) surface water supply, i.e. streamflow; (ii) total water availability, i.e. runoff; or (iii) total water withdrawals by the irrigation, industrial, and residential sectors. Note that here the 'industrial and residential sectors' refers to the withdrawals from He *et al* (2021) and not to those specifically for our agglomerations.

For these future thresholds, we require future streamflow, total water use, and total water withdrawal data. Since FLO1K only reaches up to 2015, we require another streamflow dataset to extend beyond the historical period. We apply a delta change factor to the resampled FLO1K streamflow data, using streamflow data from PCR-GLOBWB forced with ISIMIP2b (Frieler *et al* 2017, Sutanudjaja *et al* 2018) bias corrected climate data, including four different General Circulation Models (GCMs): GFDL-ESM2M; HADGEM2-ES; IPSL-CM5A-LR; and MIROC5 (Sutanudjaja *et al* 2018). We estimate future values for the FLO1K streamflow by first finding the cells in FLO1K that intersect with those in PCR-GLOBWB. Then, we take 1996–2005 as our baseline period and calculate the relative differences between each future year (2031—2070) and the baseline period within PCR-GLOBWB for each calendar month. We then apply those differences to the FLO1K values in the baseline period (equation (5)).

$$Q_{FLO1K,fut,m,y} = \frac{Q_{pib,m,y}}{\bar{Q}_{pib,m}^{1996-2005}} * \bar{Q}_{FLO1K,m}^{1996-2005} \quad (5)$$

With: Q_{FLO1K} = the streamflow from FLO1K; Q_{pib} = streamflow from PCR-GLOBWB forced with ISIMIP2b.

Runoff data from the same ISIMIP2b-forced PCR-GLOBWB model are used to determine future total water availability following the methods from section 2.2.3, but averaged over 2040–2060. Total water use is directly derived from He *et al* (2021).

Table 1. Measures that replace (produce or save) freshwater and their corresponding unit costs in 2005USD/m³. D_h and D_v, respectively are the horizontal and vertical distance between the coastline and the agglomeration border in km. Drought solving capacity refers to the percentage of the drought volume that each measure can solve.

Measures to replace lost freshwater	Unit price [2005USD/m ³] for the target agglomerations	Drought solving capacity [%]	Unit price source
Increase surface-water reservoir storage	0.12—2.52	100	Ward <i>et al</i> (2010)
Reuse urban-industrial/residential water	0.30	50	Straatsma <i>et al</i> (2020)
Increase desalination	$1.00 + 0.0006 \cdot D_h + 0.50 \cdot D_v$	100	Straatsma <i>et al</i> (2020); Zhou and Tol (2005)

2.3. Drought costs

2.3.1. Costs assessment

We convert the hazard indicator to the costs of drought to resemble the socioeconomic impacts of drought. Although large-scale drought cost assessments are limited and no dominant approach exists, Logar and Van den Berg (2013) compared drought cost assessment methods and argued that market valuation techniques are most suitable to assess drought costs for different economic sectors and require relatively low amounts of input while still holding a relatively high precision. Here we use the ‘market price method’ variant, in which the market price of a product/service is multiplied by the quantity lost to, in this case, a drought Logar and Van den Berg (2013). The product is in this case the water that needs to be gained from other sources in order to maintain business as usual under drought conditions.

Studies have been conducted in the past that used the market price method to monetize water scarcity on the global scale (Hughes *et al* 2010, Ward *et al* 2010, Straatsma *et al* 2020). They make use of several globally applicable adaptation options that replace—i.e. produce, gather or save—lost freshwater. Globally applicable unit costs of three of these adaptation measures were found in those studies that are also relevant to urban drought impact mitigation (table 1). From these measures, we derive a drought cost range per agglomeration. Note that all costs are in 2005USD, the same reference value as used in the SSP database.

2.3.2. Replacement costs calculations per measure

2.3.2.1. Increase surface water reservoir storage

The first measure, increasing surface-water reservoir storage, has a unit cost between \$0.12/m³ and \$2.52/m³, depending on the region in which they are located and their characteristics. It includes a construction, implementation, and maintenance component (Ward *et al* 2010). These costs were calculated by Ward *et al* (2010), who used a relationship between a region’s mean slope and the unit cost per m³ of 11 different reservoir-size classes. The regions used were the so-called Food Producing Units (FPUs). We calculate the unit price per agglomeration by first searching for the intersecting FPU per source location as well as the corresponding unit cost of that FPU, and subsequently averaging the costs over all source locations to derive one unit price per agglomeration.

2.3.2.2. Reuse urban industrial/residential water

The unit cost of the second measure, reuse of urban-industrial/residential water, is set to \$0.30/m³. This price includes the construction costs plus maintenance costs to maintain the measure through 2099 (Straatsma *et al* 2020).

2.3.2.3. Increase desalination

Increased desalination is composed of two parts. First, it has a constant component of \$1.00/m³ for the desalination process itself. Second, it also has a variable component to reflect the transportation costs of the water from the nearest surface salt-water body to the city border, which was set to \$0.0006/m³ per km horizontal transport and \$0.5/m³ per km vertical transport (Zhou and Tol 2005). We use the coastlines from Natural Earth V4.1.0 (naturalearthdata.com) and the agglomeration borders from GHS-SMOD (Florczyk *et al* 2019; see 2.4.1) to determine the horizontal distance as the crow flies. Furthermore, we use the SRTM Digital Terrain Model V4.1 (Reuter *et al* 2007) to determine the vertical distance along the horizontal distance line. We consider both uphill as well as downhill directions, as we assume that the brine (wastewater from desalination) needs to be transported back to its source (Jones *et al* 2019). Even if the brine is processed locally, its disposal is still a costly process, especially further inland (Brady *et al* 2005, Kesieme *et al* 2013), and this is not considered in the constant cost component (Zhou and Tol 2005). This suggests that the total price of desalination is in any case likely to be

larger than the constant component + uphill transportation costs only, which we argue to be reason to include the additional transportation costs back to the coast.

2.3.3. Cost aggregation

Since there is no specific globally uniform order in which these measures should be applied, we use a scenario approach to calculate the costs for each of these measures individually. The resulting minimum and maximum costs are then used to compose a cost range per city. These cost ranges are standardized per agglomeration by dividing them by the agglomeration's current population. Furthermore, it is assumed that the additional freshwater from increasing desalination or reservoir storage is sufficient to solve full drought volumes, since these measures could provide vast amounts of water (Lehner *et al* 2011, Jones *et al* 2019). However, even though there is no global estimate available of the potential for the reuse of urban-industrial/residential water (Paranychianakis *et al* 2015), it is capped at 50%, since several researchers showed that most countries do not have the potential to treat all of their wastewater (Anderson 2003, Paranychianakis *et al* 2015, Bauer *et al* 2020). The drought costs are thus calculated with equations (6) and (7):

$$C_{\min,a} = \begin{cases} \left(\frac{V_{\text{abs},a}}{2}\right) * P_{\text{ruw}} + \left(\frac{V_{\text{abs},a}}{2}\right) * \min(P_{\text{irs}}, P_{\text{ids}}), \& \min(P_{\text{irs}}, P_{\text{ruw}}, P_{\text{ids}}) = P_{\text{ruw}} \\ V_{\text{abs},a} * \min(P_{\text{irs}}, P_{\text{ids}}), \& \min(P_{\text{irs}}, P_{\text{ruw}}, P_{\text{ids}}) \neq P_{\text{ruw}} \& \end{cases} \quad (6)$$

$$C_{\max,a} = \begin{cases} \left(\frac{V_{\text{abs},a}}{2}\right) * P_{\text{ruw}} + \left(\frac{V_{\text{abs},a}}{2}\right) * \max(P_{\text{irs}}, P_{\text{ids}}), \& \max(P_{\text{irs}}, P_{\text{ruw}}, P_{\text{ids}}) = P_{\text{ruw}} \\ V_{\text{abs},a} * \max(P_{\text{irs}}, P_{\text{ids}}), \& \max(P_{\text{irs}}, P_{\text{ruw}}, P_{\text{ids}}) \neq P_{\text{ruw}} \& \end{cases} \quad (7)$$

With: C_{\min} = minimum drought costs; C_{\max} = maximum drought costs; a = agglomeration; V_{abs} = absolute drought volume; P_{irs} = unit price of increasing surface-water reservoir storage; P_{ruw} = unit price of reusing urban-industrial/residential water; P_{ids} = unit price of increasing desalination.

2.4. Exposure

Our exposure metric is the population totals within each agglomeration, as the CWM does not provide information on the share of citizens that is connected to the municipal water supply system. We therefore assume that all the residents in an agglomeration are potentially affected by drought, because freshwater is a scarce, widely-used, and non-substitutable economic good (van der Zaag and Savenije 2006). Larger populations lead to a smaller share of remaining water per capita, thereby increasing the drought risk. For the population data, we use data from the 30 arcseconds gridded 2UP model, which includes both current population (2010) as well as future projections towards 2050 under five different SSPs (Van Huijstee *et al* 2018). Agglomeration borders are derived from the GHS-SMOD dataset (Florczyk *et al* 2019), which builds upon a physical definition of a 'city' based on population totals and densities, following the new Degree of Urbanization (DEGURBA; Dijkstra and Poelman 2014). A physical definition of a 'city' is preferred over an administrative one in global-scale analyses, because the administrative borders are not consistently defined between different countries, whereas physical ones are (UN-DESA 2019).

The CWM contains point locations of each agglomeration, but these have no spatial borders. To use the physical-city definition, we link each CWM-agglomeration point to a GHS-SMOD agglomeration polygon, which means that, for each GHS-SMOD border, we accumulate the total drought volume from all the intersecting CWM points. To test the validity of merging agglomerations, we compared the 2010 population from 2UP within each GHS-SMOD agglomeration with that from the CWM agglomerations (McDonald *et al* 2014; UN-DESA 2019), which shows that for 92% of the GHS-SMOD agglomerations, 2UP population totals are in between halve or double the population of the CWM agglomerations (Supplementary figure S1). The CWM consists of 534 agglomerations of which we keep 264 unique urban agglomerations after filtering on agglomerations with surface water extractions, merging them in the GHS-SMOD borders, removing agglomerations with either no available 2UP data or GHS-SMOD border, and splitting them on country borders (supplementary figures S2 and S3).

2.5. Vulnerability

2.5.1. Indicator choice

To better estimate the agglomerations most at risk of a hydrological drought, we compose a vulnerability index from a set of individual indicators to operationalize and quantify those characteristics that make urban agglomerations susceptible to drought impacts. Creating an index is the most commonly applied method to assess vulnerability for drought (UNDRR 2021). We provide one vulnerability value per city, but we acknowledge that there is usually a large variability within cities (e.g. between different population groups). However, the index approach is suitable to compare cities, which is part of the goal of this paper. We base our

Table 2. Overview of the indicators and their variables for operationalization used in this study.

Indicator	Variable	Unit	Year	Weight
Access to clean water	Unimproved/No Drinking Water	% of population	2015	0.15
Poverty	Poverty	Poverty headcount ratio at \$1.90 a day (2011 PPP) (% of population)	Most recent value between 1960-2020	0.14
Water quality	Untreated Connected Wastewater	% of population	2000-2010	0.15
Government Effectiveness	Government ineffectiveness	—	2020	0.15
Conflict & insecurity	Number of conflicts	Count	Sum over 1989-2017	0.13
Sanitation	Unimproved/No Sanitation	% of urban population	2020	0.13
Groundwater depletion	Groundwater table decline	cm/year	Average change over 1990-2014	0.14

individual indicators on the work of Meza *et al* (2019), who listed and ranked a set of indicators based on the experience of a group of drought experts from different regions and with different scopes. We deem an indicator relevant if it scored equal to, or above, a relevance-score of 0.8 for drought experts with a general and a global scope. Furthermore, to ensure that multiple facets of vulnerability are considered, we also make sure that we include at least one indicator for the following set of commonly recognized vulnerability sub-dimensions: 'Social', 'Economic', 'Infrastructure', 'Environmental', 'Governance', and 'Crime & Conflict' (Gonzalez-Tanago *et al* 2016, Hagenlocher *et al* 2019, Meza *et al* 2019). If there is no indicator that belongs to a specific sub-dimension that fulfills the first criterion, then the best scoring indicator from Meza *et al* (2019) is chosen instead. For each indicator a relevant and available variable was determined, partly based on an expert interview (see Acknowledgements), resulting in the final set of indicators and variables in table 2.

2.5.2. Vulnerability index

To calculate the vulnerability index, we first determine a value for each indicator per agglomeration by intersecting each agglomeration with the spatial unit of the indicator (i.e. national, sub-national, or city level). Second, we sort the values such that the vulnerability increases with the indicator value. Third, we standardize each indicator based on min-max normalization. Finally, each standardized indicator is given a weight, based on the overall relevance score in Meza *et al* (2019, table 2), and is aggregated in the vulnerability index (Supplementary table S1). Note that these weights are close to the weights that would be obtained with equal weighting ($1/7 = \sim 0.143$), because the individual relevance scores from Meza *et al* (2019) are relatively close to each other. Hence, the indicators have approximately the same relevance, although Access to clean water, Government effectiveness, and Water quality are considered slightly more important.

Unimproved/No Drinking Water indicates which part of the population has to fetch water from unprotected sources (Hofste *et al* 2019). This makes them vulnerable during drought as lower water levels increase the density of pathogens in the water. **Poverty** denotes the percentage of people earning below living standards (World Bank 2022). This limits them to undertake adaptations to drought and to financially respond to drought damage. **Untreated Connected Wastewater** denotes the amount of water that flows through the sewers without any level of treatment (Hofste *et al* 2019). Again, this increases pathogen concentrations in the water during drought. **Government effectiveness** captures several governance-related indicators into one index that measures the perception of the quality of, among others, public services, policy formulation and implementation, and government credibility (Kaufmann *et al* 2011). It affects the efficiency in which a government deals with drought (see for instance Simpson *et al* 2019). It is deemed especially suitable for cross-country comparison at larger geographical scales (Kaufmann *et al* 2011). **Number of conflicts** shows the sum of individual organized violent conflicts for a city (Sundberg and Melander 2013, Davies *et al* 2022). This is an indication of the unrest and therefore the lack of cooperation on disaster risk reduction within a city. **Unimproved/No Sanitation** refers to the amount of people that do not have access to more than very basic sanitation structures (Hofste *et al* 2019, WHO and UNICEF 2021). Human feces can accumulate in the urban environment during drought, causing potential health issues. **Groundwater table Decline** measures how much the water table changes in groundwater sources (Hofste *et al* 2019). This decreases the capability to resort to groundwater sources when surface water sources run dry. More information on the sources and acquisition of this data can be found in supplementary table S2.

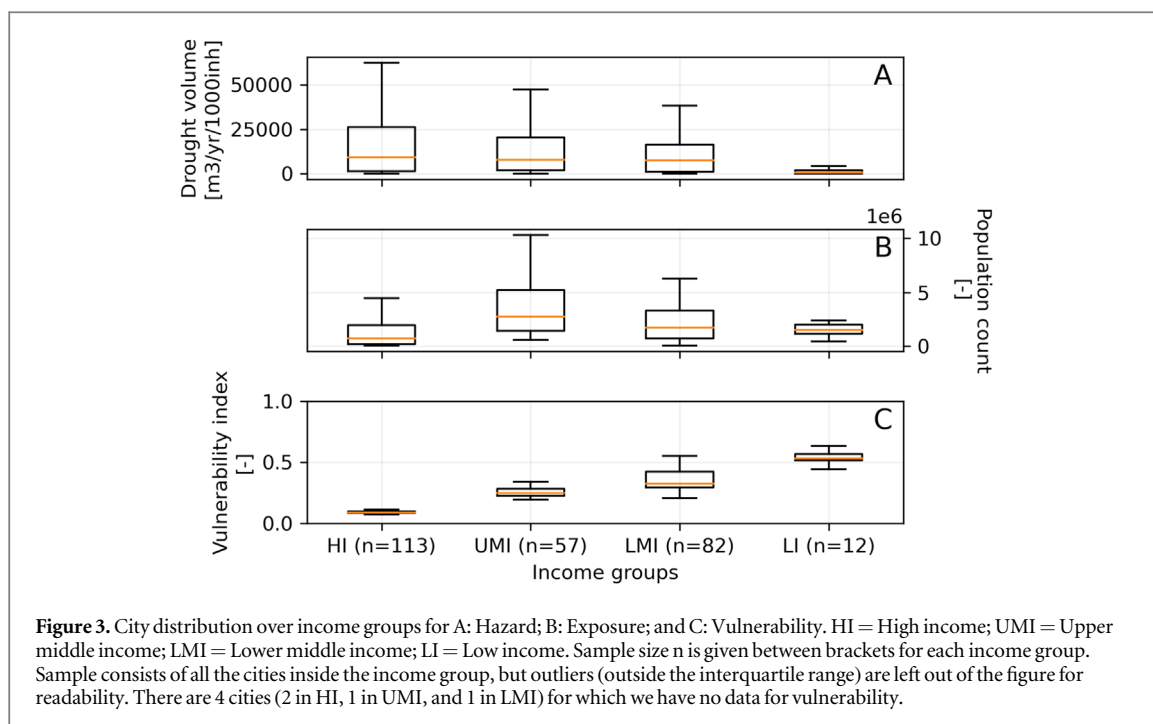
2.6. Risk

We derive the risk for the historical period (1971-2010) as well as for the future period (2031-2070) under the SSP1+RCP2.6 and SSP3+RCP6.0 projections. We cannot attach an overall risk number on the absolute drought risk per individual city, but by making combinations of costs and vulnerability categories we are able to identify nine risk profiles. These profiles are based on the 33th (low), 66th (medium) and 100th (high) percentiles of cost and vulnerability values. We use a trivariate map that is composed of (i) a bivariate choropleth that shows these nine drought risk categories and (ii) a proportional symbol map that adds exposure. We then assess the total number of agglomerations and their exposure within each risk category as well as their evolution over time, to quantify the change in risk over time.

3. Results

3.1. Global patterns

Figure 3 shows our cities' hazard, exposure and vulnerability distribution over the historical period, aggregated into income categories: High income (HI), Upper middle income (UMI), Lower middle income (LMI), and Lower income (LI) (Fantom and Serajuddin 2016). The average hazard is similar for HI, UMI, and LMI, but is, within our set of cities, substantially lower for LI (figure 3(a)). Moreover, the range of the hazard is inversely

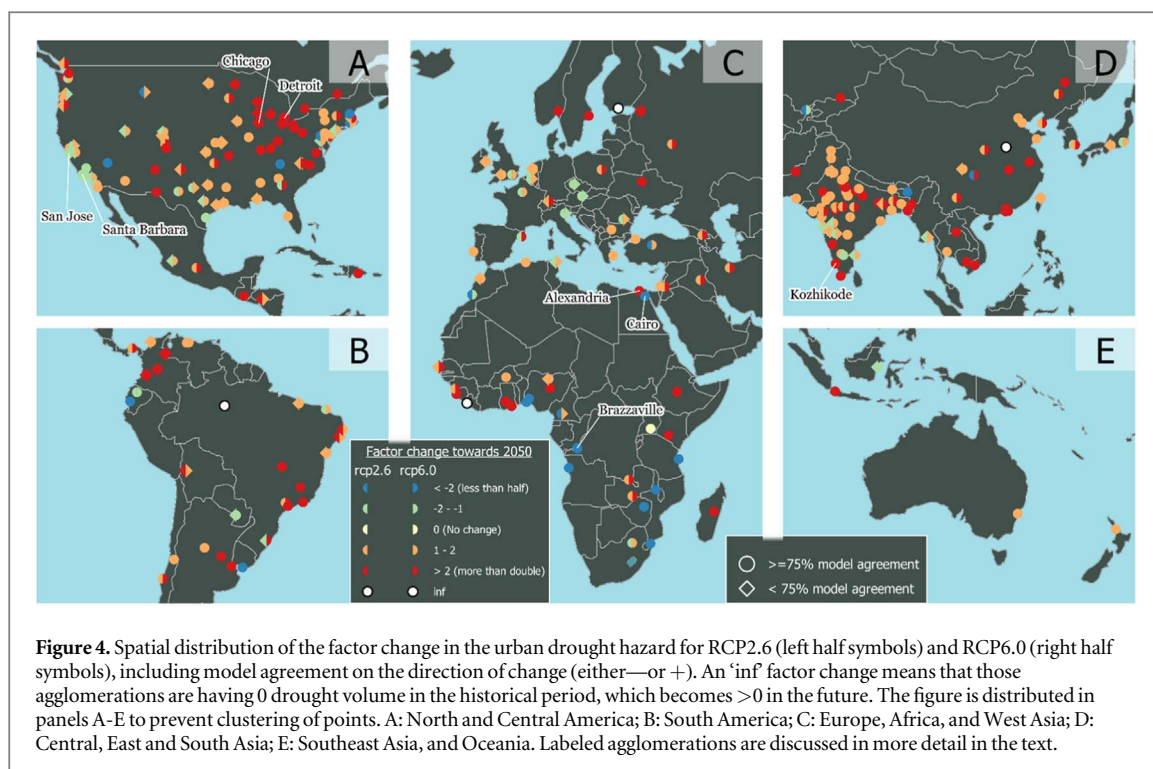


correlated with income in our data, which indicates that there is less variation in the hazard in LI than HI cities. However, it should be noted that the LI group only has 12 cities which are all on the African continent in tropical or temperate climates and this may limit the variability in this group. The most exposed cities are found in the UMI and LMI groups, which are likely economic developing countries that rapidly grow in size or have grown in size over the past years (figure 3(b); Bauch 2008). The vulnerability index shows an inverse trend with income in our data. Our individual vulnerability indicators do likely favor higher income cities, as there is likely more investment opportunities in for instance sanitation and water supply in wealthier cities (figure 3(c)). The remainder of this chapter discusses the spatial distribution of the hazard, exposure and vulnerability. See the supplement for more Figures on these components for the different time periods (Supplementary Figures S4, S5, S6, S10, and S11).

3.2. Hazard

Our estimates shows that the median standardized urban drought hazard increases towards 2050 with 66%: from $\sim 8,000\text{m}^3/\text{year}$ per 1000 citizens to $\sim 10,000\text{--}13,000\text{m}^3/\text{year}$ per 1000 citizens (supplementary figure S7). This increase is significant at $p < 0.05$ following the Wilcoxon Sign-Ranked-Test (Wilcoxon 1945). In addition, 73% and 88% of the agglomerations have a projected increase in annual average drought volumes over time for RCP2.6 and RCP6.0 respectively. Figure 4 presents this spatially and also shows the model agreement on the sign of change—either an increase, decrease or no change. Note that the drought costs have the same factor change as the drought hazard, since the unit costs remain static over time. With the methodology used in this study, an agglomeration's hydrological drought volume or costs can change with time if either the drought threshold or the climate variability changes. This can be analyzed by looking at changes in (i) the WSI; (ii) the drought frequency (i.e. the threshold exceedance frequency); and (iii) the drought intensity (i.e. the average threshold-exceedance volume).

Based on our model, strong relative increases occur mostly in northern India, Pakistan, the Midwestern US, eastern Brazil, and most of western Africa (figure 4). The drought hazard is already large in our historical simulation for northern India and Pakistan and is thus projected to worsen in the future there, mostly with $>75\%$ model agreement. We have found the biggest drought hazard in San Diego (United States); Los Angeles (United States); and Quetta (Pakistan). Both San Diego and Los Angeles extract relatively large volumes of water from several source locations—of which some are shared between them. The mean WSI for San Diego's source locations is close to 1, implying that most of the water at those locations is already assigned to a purpose. Historically, the drought threshold is therefore exceeded 81% and 78% of the time for San Diego and Los Angeles respectively, which mostly explains the large drought hazard. Quetta, the agglomeration with the third-largest drought volume, has lower WSI values than San Diego and Los Angeles in the historical time period, but this difference shrinks towards the future. Also, Quetta's drought frequency increases towards 2050, which



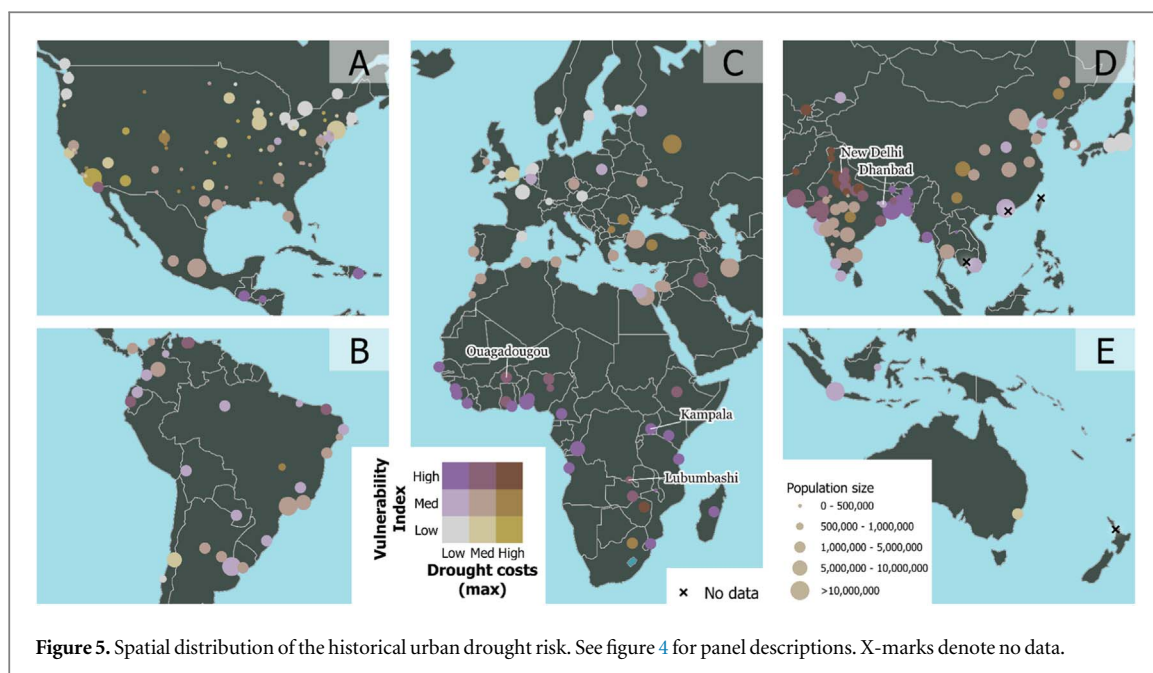
altogether results in a doubling in drought volume under both RCPs for this agglomeration (supplementary table S3).

On the other side of the spectrum, some agglomerations in parts of southern Africa experience a decrease in hazard towards 2050 according to our model. We also observe this at the west coast of the US for some agglomerations with large historical urban drought volumes (e.g. San Jose and Santa Barbara; figure 4). Five agglomerations have no urban drought hazard in the historical situation: Manaus (Brazil), Monrovia (Liberia), Helsinki (Finland), Kampala (Uganda), and Zhengzhou (China). From these, only Kampala remains free of drought in 2050 for both RCPs. The low volumes are predominantly caused by the WSI, which is close to 0 for these agglomerations. The drought frequency does not increase much towards 2050 in most of these agglomerations, with Manaus having the highest threshold exceedance frequency with 10%. However, the drought intensity rises strongly for Manaus and Zhengzhou, and it is therefore likely that the increase in drought hazard is due to the local streamflow becoming either more erratic over time or overall less on average towards 2050 for these agglomerations (supplementary table S3).

Figure 4 also shows us that there is a larger model agreement for RCP6.0 compared to RCP2.6. This is especially evident in the Midwestern US (e.g. Chicago and Detroit), where the strong increase in drought volume is backed only by a 50% model agreement for RCP2.6. Here, the increase of two models outweighs the decrease in the other two. This indicates that for some parts of the world our model identifies high levels of uncertainty in future drought conditions, especially under RCP2.6 (supplementary figure S8). Strong changes in the hazard can be found in arid agglomerations like Alexandria and Cairo. However, we should handle these cities with care, because both FLO1K and PCR-GLOBWB show relatively large uncertainties in arid regions (Sperna-Weiland *et al* 2010, Barbarossa *et al* 2018). Outside arid regions, Brazzaville (Republic of the Congo) shows a strong decrease with factor changes of -18 (RCP2.6) and -33 (RCP6.0) due to a decrease in the frequency of drought occurrences. Kozhikode (India) has strong positive factor changes of 13 (RCP2.6) and 34 (RCP6.0), mainly due to an increase in the WSI (supplementary table S3).

3.3. Exposure and vulnerability

Our results indicate that exposure will increase over time for almost 97% of the agglomerations in SSP1, and for 91% of the agglomerations in SSP3 (supplementary figure S10). For SSP1, the top 20 agglomerations with the largest increase in population are exclusively in Sub-Saharan Africa and central and western India. From the 2UP population data, we find the largest increase in Kampala (x4.0; Uganda), which does not have any urban drought hazard and is thus not exposed, followed by Dhanbad (x3.4; India) and Ouagadougou (x3.4; Burkina Faso). For SSP3, all but one of the fastest growing agglomerations are again in Sub-Saharan Africa and Western Asia, with the top 3 consisting of Kampala (x3.4), Lubumbashi (x2.7; Democratic Republic of the Congo), and Ouagadougou (x2.7). Decreasing populations are mostly found in agglomerations across Europe and East Asia.



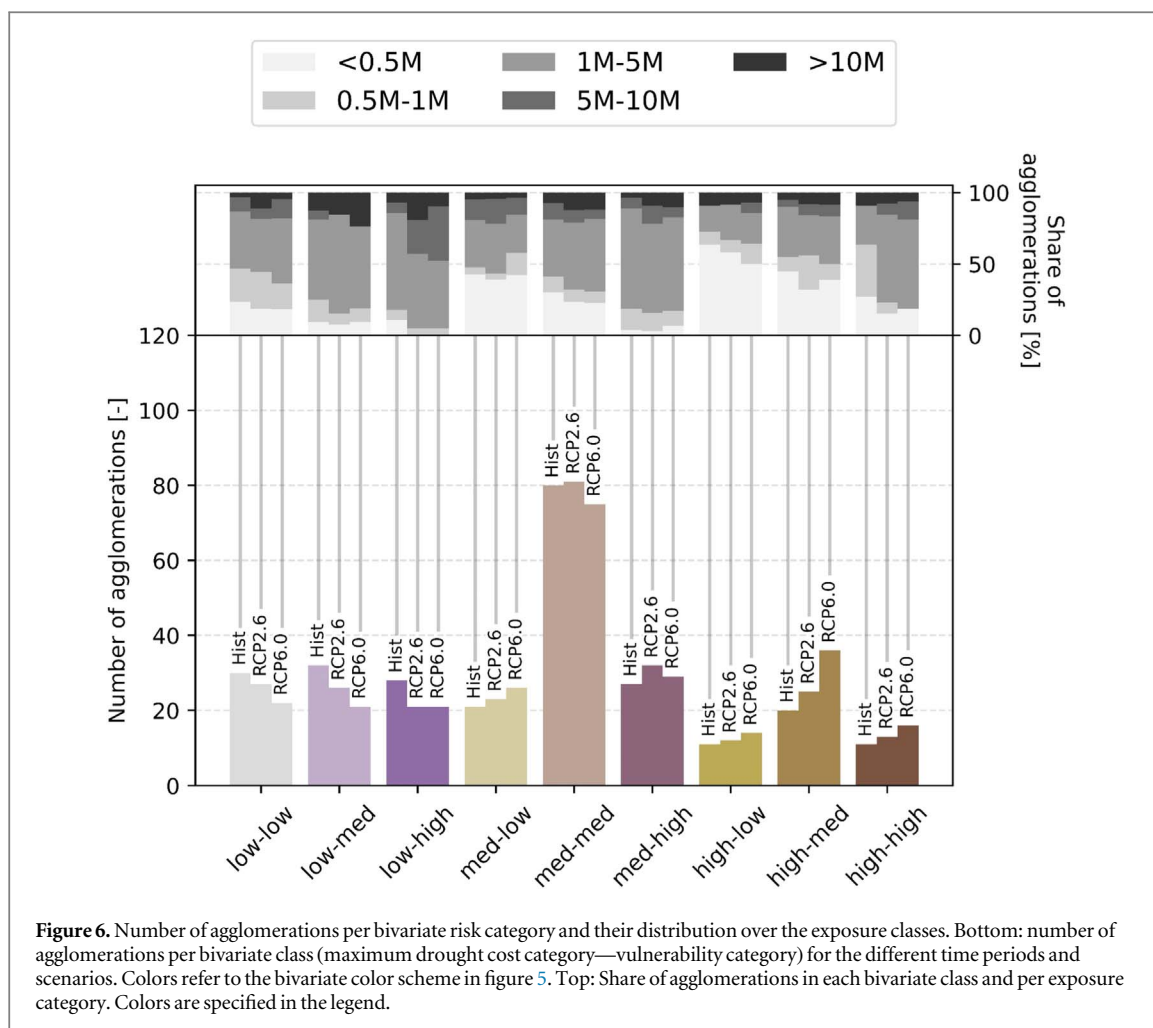
Agglomerations with the largest vulnerability in our model can be found in similar regions (supplementary figure S11). Here, agglomerations score high on large shares of untreated connected wastewater. Next to that, most sub-Saharan African agglomerations score relatively high on the variables government ineffectiveness, unimproved/no drinking water, and poverty. The large vulnerability in northern Indian agglomerations is accompanied by large groundwater table declines. Agglomerations in Central and South Asia also have to deal with relatively medium to high values for the government ineffectiveness variable. Thus, vulnerability profiles differ amongst agglomerations with similar scores, although untreated connected wastewater and government ineffectiveness are often the most influential in these cases. The least vulnerable agglomerations are in northern and western Europe, the US, Australia, southern South America, and Japan.

3.4. Risk

Figure 5 shows the trivariate risk map for the historical situation (see supplementary Figures S12-13 for RCP2.6 and RCP6.0). The agglomerations that are arguably most at risk in our model are those located in Central and South Asia. These have high vulnerability and medium/high drought costs, although they mostly fall in the lowest three exposure classes (figure 6). The agglomeration in the highest categories of drought costs and vulnerability, as well as with the largest exposure class (>10M), is New Delhi, which we therefore consider to be the agglomeration most at risk from urban droughts, both historically as in the projected futures. In fact, New Delhi has recently experienced several droughts with severe consequences (Bhardwaj 2019; Delhi News 2022).

In contrast, agglomerations in Europe, along the United States-Canadian border, and—to a lesser extent—the remainder of Asia have low/medium vulnerability and costs alike and could be considered to have the lowest urban drought risk according to our model. Other regions have low/medium vulnerability, but have to deal with larger drought costs (North America, and the Mediterranean), or conversely have high vulnerability with low/medium drought costs (Sub-Saharan Africa). These regions have a large share of agglomerations with population totals exceeding 1M (figure 6), and are thus prone to shifting to the highest risk class if either the drought costs or the vulnerability would increase. The most diverse region in terms of risk profiles is South America, which includes agglomerations over the whole range of vulnerability classes and with low/medium costs.

Towards 2050, spatial patterns stay mostly the same, but several agglomerations shift between drought risk categories. Figure 6 shows that the share of agglomerations in the lowest cost class decreases, whereas the number of agglomerations in the highest cost class increases. Yet, the medium/medium class has the largest share of agglomerations (~30%) in all time periods and scenarios. Moreover, for almost all bivariate classes, exposure increases towards 2050, as an increasing share of agglomerations will have a population exceeding 1M. Yet, the share of agglomerations with low exposure remains larger in the high-cost classes than in the low-cost classes. Lastly, figure 6 also shows that exposure is increasing with vulnerability.



4. Discussion

4.1. Assumptions and the way forward

In this study, we took a novel approach to get a first estimate of global urban drought risk. The results can be used to make comparisons across cities and to find larger geographical trends of drought hazard/costs, exposure, vulnerability and risk. A global-scale approach comes inevitably with several—sometimes major—assumptions due to a lack of data. We should therefore be careful in deriving detailed city-level implications from our model. Here we discuss two main assumptions, how they likely influence our results, and how we can improve this in future research.

In our analysis, we did not cover for groundwater abstractions in the hazard due to modeling complexities. As such, it may be possible that agglomerations experience lower drought hazard than suggested in our results, because they still have access to sufficient groundwater sources. Flörke *et al* (2018) examined the urban groundwater footprint—the ratio of urban water withdrawals from groundwater to the groundwater recharge rate—and found that all cities (apart from some in Europe) are expected to have a higher footprint in the future than they have now. In other words, these groundwater sources are increasingly stressed and may thus not be sustainable in the long run. Yet, future research may yield more robust results when including groundwater, as it is an important resource for cities (McDonald *et al* 2014).

Furthermore, we assumed constant withdrawal rates over time for each agglomeration, based on the CWM data, but in reality these rates can change with several aspects, for example population, economic profiles, and technology (McDonald *et al* 2011, Kuil *et al* 2019). Wada *et al* (2016) compared total withdrawals for several global hydrological models that considered some of these aspects. They did this for different SSPs and water use sectors, including the domestic and industrial sectors, which are the ones that potentially make use of the municipal water supply as considered in the CWM (McDonald *et al* 2014 and 2016, personal correspondence). They found that, by 2050, domestic water use could change by between +40% and +170% for SSP1, and between +90% and +250% for SSP3, and that industrial water use could change between −40% and +100% for SSP1, and between +45% and +120% for SSP3. Hence, if we were to account for these changing urban

withdrawal rates as well as for the previous assumption on groundwater, the drought hazard would most likely increase even further towards the future, compared to what we found in our own results. A potentially promising avenue to explore this gap are the use of SSPs in future projections of socioeconomic circumstances (Wilts *et al* 2021).

4.2. Implications for cities

The drought risk hotspots from this study can guide city-level or regional-scale studies on urban drought. Using local information, such in-depth studies can further specify the drought hazard and population exposed, as well as identify the most vulnerable parts of the local urban system. More specifically, as we have outlined in this paper, cities need to inventory their water sources, map the variability in water, identify who is affected by drought, and unravel the local complexities that make up their vulnerability. Furthermore, the urban drought risk profiles can raise awareness to drought amongst cities and aid urban-focused transnational climate action groups like C40 or R-Cities to identify cities in similar circumstances. It should also be noted that not only cities that are currently experiencing large urban drought risk, but also the ones that are projected to experience increased urban drought risk in the future require further attention. Altogether, such local-scale risk assessments can in turn be used to find suitable adaptation options for specific cities.

What makes an adaptation option suitable depends for a large part on the vulnerability of the city to drought and other hazards (De Ruiter *et al* 2020). Vulnerability in turn is considered highly dynamic and strongly influenced by local circumstances (O'Brien *et al* 2007); thus the local context is critical when considering urban drought adaptation options. Note that the measures that we used to proxy the drought costs are not always the most optimal solutions, because they have several drawbacks, such as high energy intensities, ecological and environmental damage, and land cover degradation (Ahmed and Anwar 2012, Gouldson *et al* 2015, Cremades *et al* 2021, Singh *et al* 2021, Van Vliet *et al* 2021). Instead, it is recommended that cities adopt a mix of options, distinguishing between: i) reactive adaptation, focusing on the immediate impacts from extreme weather, without changing the city's systems; ii) incremental adaptation, driving adjustments to the existing city systems, building their resilience, while minimizing negative climate change impacts; and iii) transformational adaptation, aiming to reduce the root causes of climate risks, by transforming the city's systems into more just, sustainable, or resilient states (European Environment Agency 2016). Thinking about transformational adaptation strategies may help cities in identifying solutions that are sustainable in the long term and that offer opportunities for co-benefits. Under the right political, institutional, and financial circumstances, certain (transformative) adaptive measures can even provide an economic benefit (Gouldson *et al* 2015). Even if an adaptation measure is not profitable, Van den Bergh *et al* (2010) and Cartwright *et al* (2013) argue that we should look beyond the economic consequences towards the ability of adaptation and mitigation measures to increase our overall welfare and quality of life. Moreover, there is an increasing number of cities that have started to see adaptation as an opportunity to increase their attractiveness as livable cities (European Environment Agency 2016, Boon *et al* 2021).

Short-term actions that lead to quick economic gain may cloud long-term visions of politicians and planners (Buurman *et al* 2017), regardless of the benefits discussed above. On a more positive note, cities are often praised for their active response against climate change in general. Cities often have a mandate and relatively small geographical area to operate on, making them more effective in handling climate change and pushing for action than for instance nation states (Rozenzweig *et al* 2010, Johnson 2018). Cities do this both on their own or in one of the many urban-focused climate action groups (see e.g. Haupt and Coppola 2019). Barriers remain in the form of difficult integrations of climate related policies in other urban agendas and lacking support of national governments (Gouldson *et al* 2015), but adaptation and mitigation are increasingly more intertwined in city climate action plans (Grafakos *et al* 2019). There is extensive literature examining the co-benefits between adaptation and mitigation and the need to move away from compartmentalizing approaches is well recognized (Sharifi 2021).

5. Conclusion

In this study, we examined global urban drought risk in the present as well as under future projections. Using drought hazard, costs, exposure, and vulnerability, we developed urban drought risk profiles for 264 urban agglomerations and identified several hotspots around the globe, the most notable being Central and South Asia. We found 3 key results:

- We project that, towards 2050, hazard/costs increase for 73%-88% of our target agglomerations, and ...
- ...that exposure increases for 91%-97%.

- Following our model, the number of agglomerations with high costs and medium exposure increases, whilst agglomerations with low costs and low exposure reduce in number.

Our model therefore implies that urban drought risk will evolve from an already substantial threat now towards an even bigger issue in the near future.

Our results also show that urban drought is not confined to specific geographical areas and that cities across the globe should consider it as a serious threat to their functioning. Even cities that are currently not dealing with drought may need to put urban drought on their agenda to prevent it from becoming an issue in a climatic and socially changing future. Cities that already do consider drought as a threat, often deal with it in a reactive manner without considering incremental or transformational options—which is both unethical (because of human suffering) and more expensive (e.g. last minute imports from abroad, emergency aid). Cities need to act on several fronts to reduce this risk; they need to improve their water management, reduce vulnerability, and apply a balanced mix of reactive, adaptive, and transformative measures to minimize their urban drought risk and to prevent large-scale social and economic consequences.

We have also identified several avenues for future research. One avenue is to use local-scale context and data to investigate the cities from the hotspots identified in our research in more depth, for instance by applying a downscaled version of our model. Such studies may benefit from the inclusion of groundwater, dynamic city-level withdrawal rates, dynamic vulnerability indicators, information on water sources on a sub-city scale, and local information on the replacement costs of freshwater.

We have demonstrated here that drought is not solely an agricultural issue, but also an urban one. Although we estimate that urban drought risk increases for many cities in the next three decades, we also see traction in urban drought research as well as in the influence of cities on the international disaster risk management stage. If we maintain this momentum, we may still mitigate some of the urban drought risk to prevent worse impacts than those already experienced in the recent past by cities like New Delhi and Cape Town.

Acknowledgments

The authors would like to thank Rebecca Ilunga, urban drought expert at C40 cities, for her expertise on local-scale urban drought events and their consequences, which she shared with us in an expert interview. We would also like to acknowledge the Water Safe Cities project, in which we developed the first version of the urban drought risk methodology, and via which we got the opportunity to talk to city-practitioners from several cities on their experience with urban hydrological drought. Lastly we want to thank both Dr Robert McDonald and Dr Zhifeng Liu for answering our complementary questions to their respective articles.

Data availability statement

The data that support the findings of this study will be openly available following an embargo at the following URL/DOI: <https://figshare.com/s/a12572f74bf234da7369>. Data will be available from 1 May 2023.

Funding

PW, HM, FV, and TS received funding under the Water Safe Cities project from the C40 Cities Climate Leadership Group.

PW and EK received additional funding under the MYRIAD-EU project. MYRIAD-EU received funding from the European Union's Horizon 2020 research and innovation program (grant agreement no. 101003276).

Declaration of interest




The authors declare that they have no known competing financial interests or personal relationships that could have appeared to influence the work reported in this paper.

ORCID iDs

Tristian R Stolte  <https://orcid.org/0000-0002-8776-9896>

Hans de Moel  <https://orcid.org/0000-0002-6826-1974>

Elco E Koks  <https://orcid.org/0000-0002-4953-4527>

Marthe L K Wens  <https://orcid.org/0000-0002-0133-5924>
Felix van Veldhoven  <https://orcid.org/0000-0001-9671-6537>
Philip J Ward  <https://orcid.org/0000-0001-7702-7859>

References

- Acuto M, Parnell S and Seto K C 2018 Building a global urban science *Nature Sustainability* **1** 2–4
- Ahmed M and Anwar R 2012 An Assessment of the Environmental Impact of Brine Disposal in Marine Environment *International Journal of Modern Engineering Research* **2** 2756–61
- Anderson J 2003 The environmental benefits of water recycling and reuse *Water Science and Technology: Water Supply* **3** 1–10
- Arias P A et al 2021 Technical summary *Climate Change 2021: The Physical Science Basis. Contribution of Working Group I to the Sixth Assessment Report of the Intergovernmental Panel on Climate Change* (Cambridge, United Kingdom and New York, NY, USA: Cambridge University Press) pp 33–144
- Arnell N W, Lowe J A, Lloyd-Hughes B and Osborn T J 2018 The impacts avoided with a 1.5 °C climate target: A global and regional assessment *Clim. Change* **147** 61–76
- Barbarossa V, Huijbregts M A J, Beusen A H W, Beck H E, King H and Schipper A M 2018 FLO1K, global maps of mean, maximum and minimum annual streamflow at 1 km resolution from 1960 through 2015 *Scientific Data* **5** 180052
- Bauch C T 2008 Wealth as a source of density dependence in human population growth *Oikos* **117** 1824–32
- Bauer S, Linke H J and Wagner M 2020 Combining industrial and urban water-reuse concepts for increasing the water resources in water-scarce regions *Water Environ. Res.* **92** 1027–41
- van den Bergh J C J M 2010 Safe climate policy is affordable-12 reasons *Clim. Change* **101** 339–85
- Bhardwaj M 2019 In drought-hit Delhi, the haves get limitless water, the poor fight for every drop Reuters (<https://reuters.com/article/us-india-water-insight-idUSKCN1U203K>)
- Boon E, Goosen H, van Veldhoven F and Swart R 2021 Does transformational adaptation require a transformation of climate services? *Frontiers in Climate* **3** 615291
- Brady P V, Kottenstette R J, Mayer T M and Hightower M M 2005 Inland desalination: challenges and research needs *Journal of Contemporary Water Research & Education* **132** 46–51
- Buurman J, Mens M J P and Dahm R J 2017 Strategies for urban drought risk management: A comparison of 10 large cities *Int. J. Water Resour. Dev.* **33** 31–50
- Carrão H, Naumann G and Barbosa P 2016 Mapping global patterns of drought risk: An empirical framework based on sub-national estimates of hazard, exposure and vulnerability *Global Environ. Change* **39** 108–24
- Cartwright A, Blignaut J, De Wit M, Goldberg K, Mander M, O'Donoghue S and Roberts D 2013 Economics of climate change adaptation at the local scale under conditions of uncertainty and resource constraints: The case of Durban, South Africa *Environment and Urbanization* **25** 139–56
- Cremades R, Sanchez-Plaza A, Hewitt R J, Mitter H, Baggio J A, Olazabal M, Broekman A, Kropf B and Tudose N C 2021 Guiding cities under increased droughts: The limits to sustainable urban futures *Ecol. Econ.* **189** 107140
- Davies S, Pettersson T and Öberg M 2022 Organized violence 1989–2021 and drone warfare *Journal of Peace Research* **59** 593–610
- Delhi News 2022 Yamuna water level lowest since 1965, most areas in Delhi to face crisis *Hindustan Times* (<https://hindustantimes.com/cities/delhi-news/yamuna-water-level-lowest-since-1965-most-areas-to-face-crisis-101656527881928.html>)
- Desbureaux S and Rodella A S 2019 Drought in the city: the economic impact of water scarcity in Latin American metropolitan areas *World Development* **114** 13–27
- de Ruiter M C, Couasnon A, van den Homberg M J C, Daniell J E, Gill J C and Ward P J 2020 Why we can no longer ignore consecutive disasters *Earth's Future* **8** 19
- Dijkstra L and Poelman H 2014 A harmonised definition of cities and rural areas: The new degree of urbanisation *In Regional and Urban Policy* (European Commission)
- Dracup J A, Lee K S and Paulson E G 1980 On the definition of droughts *Water Resour. Res.* **16** 297–302
- European Environment Agency 2016 *Urban adaptation to climate change in Europe 2016: Transforming cities in a changing climate* (European Environment Agency) (<https://doi.org/10.2800/021466>)
- Fantom N and Serajuddin U 2016 *The World Bank's Classification of Countries by Income* (World Bank) (<https://doi.org/10.1596/1813-9450-7528>)
- Florczyk A J et al 2019 *GHSL Data Package 2019* 38 Joint Research Centre
- Flörke M, Schneider C and McDonald R I 2018 Water competition between cities and agriculture driven by climate change and urban growth *Nature Sustainability* **1** 51–8
- Frieler K et al 2017 Assessing the impacts of 1.5°C global warming—Simulation protocol of the Inter-Sectoral Impact Model Intercomparison Project (ISIMIP2b) *Geoscientific Model Development* **10** 4321–45
- Gerten D, Hoff H, Rockström J, Jägermeyr J, Kummu M and Pastor A V 2013 Towards a revised planetary boundary for consumptive freshwater use: Role of environmental flow requirements *Current Opinion in Environmental Sustainability* **5** 551–8
- González Tánago I, Urquijo J, Blauhut V, Villarroya F and De Stefano L 2016 Learning from experience: a systematic review of assessments of vulnerability to drought *Nat. Hazards* **80** 951–73
- Gouldson A, Colenbrander S, Sudmant A, McAnulla F, Kerr N, Sakai P, Hall S, Papargyropoulou E and Kuylenstierna J 2015 Exploring the economic case for climate action in cities *Global Environ. Change* **35** 93–105
- De Graaf I E M, Sutanudjaja E H, Van Beek L P H and Bierkens M F P 2015 A high-resolution global-scale groundwater model *Hydrol. Earth Syst. Sci.* **19** 823–37
- Grafakos S, Trigg K, Landauer M, Chelleri L and Dhakal S 2019 Analytical framework to evaluate the level of integration of climate adaptation and mitigation in cities *Clim. Change* **154** 87–106
- Grant S B, Fletcher T D, Feldman D, Saphores J D, Cook P L M, Stewardson M, Low K, Burry K and Hamilton A J 2013 Adapting urban water systems to a changing climate: Lessons from the millennium drought in southeast Australia *Environ. Sci. Technol.* **47** 10727–34
- Gu D 2019 *Exposure and vulnerability to natural disasters for world's cities* Technical paper 4 1–43
- Guerreiro S B, Dawson R J, Kilsby C, Lewis E and Ford A 2018 Future heat-waves, droughts and floods in 571 European cities *Environ. Res. Lett.* **13** 10034009
- Güneralp B, Güneralp I and Liu Y 2015 Changing global patterns of urban exposure to flood and drought hazards *Global Environ. Change* **31** 217–25

- Guo H, Zhang X, Lian F, Gao Y, Lin D and Wang J 2016 Drought risk assessment based on vulnerability surfaces: a case study of maize *Sustainability (Switzerland)* **8** 22813
- Hagenlocher M, Meza I, Anderson C C, Min A, Renaud F G, Walz Y, Siebert S and Sebesvari Z 2019 Drought vulnerability and risk assessments: State of the art, persistent gaps, and research agenda *Environ. Res. Lett.* **14** 083002
- Haqiqi I, Grogan D S, Hertel T W and Schlenker W 2021 Quantifying the impacts of compound extremes on agriculture *Hydrol. Earth Syst. Sci.* **25** 551–64
- Haupt W and Coppola A 2019 Climate governance in transnational municipal networks: Advancing a potential agenda for analysis and typology *International Journal of Urban Sustainable Development* **11** 123–40
- He C, Liu Z, Wu J, Pan X, Fang Z, Li J and Bryan B A 2021 Future global urban water scarcity and potential solutions *Nat. Commun.* **12** 1–11
- Hofste R et al 2019 Aqueduct 3.0: updated decision-relevant global water risk indicators *World Resources Institute*
- Hsiang S M, Burke M and Miguel E 2013 Quantifying the influence of climate on human conflict *Science* **341** 1235367
- Huang Z, Yuan X and Liu X 2021 The key drivers for the changes in global water scarcity: Water withdrawal versus water availability *J. Hydrol.* **601** 126658
- Hughes G, Chinowsky P and Strzepek K 2010 The costs of adaptation to climate change for water infrastructure in OECD countries *Util. Policy* **18** 142–53
- IPCC 2014 *Climate Change 2014: Synthesis Report. Contribution of Working Groups I, II and III to the Fifth Assessment Report of the Intergovernmental Panel on Climate Change* ed Core Writing Team, R K Pachauri and L A Meyer (Geneva, Switzerland: IPCC) p 151
- Johnson C A 2018 Taking It to the Streets (and Beyond): The Power of Cities in Global Climate Politics *The Power of Cities in Global Climate Politics* (London: Palgrave Macmillan London) (*Cities and the Global Politics of the Environment*) 1st ednch 5 pp 147–58
- Jones E, Qadir M, van Vliet M T H, Smakhtin V and Kang S mu 2019 The state of desalination and brine production: A global outlook *Sci. Total Environ.* **657** 1343–56
- Kaufmann D, Kraay A and Mastruzzi M 2011 The Worldwide Governance Indicators: Methodology and Analytical Issues *Hague Journal on the Rule of Law* **3** 220–246
- Kesime U K, Milne N, Aral H, Cheng C Y and Duke M 2013 Economic analysis of desalination technologies in the context of carbon pricing, and opportunities for membrane distillation *Desalination* **323** 66–74
- Kron W 2005 Flood risk = hazard • values • vulnerability *Water Int.* **30** 58–68
- Kuil L, Carr G, Prskawetz A, Salinas J L, Viglione A and Blöschl G 2019 Learning from the ancient maya: exploring the impact of drought on population dynamics *Ecol. Econ.* **157** 1–16
- Lehrer B et al 2011 High-resolution mapping of the world's reservoirs and dams for sustainable river-flow management *Frontiers in Ecology and the Environment* **9** 494–502
- Liu Y and Chen J 2021 Future global socioeconomic risk to droughts based on estimates of hazard, exposure, and vulnerability in a changing climate *Sci. Total Environ.* **751** 142159
- Liu Z, He C, Zhou Y and Wu J 2014 How much of the world's land has been urbanized, really? A hierarchical framework for avoiding confusion *Landscape Ecology* **29** 763–71
- Logar I and van den Bergh J C J M 2013 Methods to assess costs of drought damages and policies for drought mitigation and adaptation: review and recommendations *Water Resour. Manage.* **27** 1707–20
- Masutomi Y, Inui Y, Takahasi K and Matsuoka Y 2009 Development of highly accurate global polygonal drainage basin data *Hydrol. Processes* **23** 572–84
- McDonald R I et al 2014 Water on an urban planet: Urbanization and the reach of urban water infrastructure *Global Environ. Change* **27** 96–105
- McDonald R I, Green P, Balk D, Fekete B M, Revenga C, Todd M and Montgomery M 2011 Urban growth, climate change, and freshwater availability *PNAS* **108** 6312–7
- McDonald R I, Weber K F, Padowski J, Boucher T and Shemie D 2016 Estimating watershed degradation over the last century and its impact on water-treatment costs for the world's large cities *PNAS* **113** 9117–22
- McPhearson T, Parnell S, Simon D, Gaffney O, Elmqvist T, Bai X, Roberts D and Revi A 2016 Scientists must have a say in the future of cities *Nature* **538** 165–6
- Meza I et al 2020 Global-scale drought risk assessment for agricultural systems *Natural Hazards and Earth System Sciences* **20** 695–712
- Meza I, Hagenlocher M, Naumann G, Vogt J V and Frischen J 2019 *Drought Vulnerability Indicators for Global-Scale Drought Risk Assessments—Global Expert Survey Results Report* (Publications Office of the European Union) pp 1–62
- Mishra A K and Singh V P 2010 A review of drought concepts *J. Hydrol.* **391** 202–16
- Natural Earth (n.d.). *Naturalearthdata*. Retrieved July 1, 2021, from (<https://naturalearthdata.com/>)
- Naumann G, Cammalleri C, Mentaschi L and Feyen L 2021 Increased economic drought impacts in Europe with anthropogenic warming *Nat. Clim. Change* **11** 485–91
- Nobre C A, Marengo J A, Seluchi M E, Cuartas L A and Alves L M 2016 Some characteristics and impacts of the drought and water crisis in southeastern Brazil during 2014 and 2015 *J. Water Resour. Prot.* **08** 252–62
- O'Brien K, Eriksen S, Nygaard L P and Schjolden A 2007 Why different interpretations of vulnerability matter in climate change discourses *Climate Policy* **7** 73–88
- O'Neill B C, Krieglger E, Riahi K, Ebi K L, Hallegatte S, Carter T R, Mathur R and van Vuuren D P 2014 A new scenario framework for climate change research: The concept of shared socioeconomic pathways *Clim. Change* **122** 387–400
- Paranychianakis N V, Salgot M, Snyder S A and Angelakis A N 2015 Water reuse in EU states: Necessity for uniform criteria to mitigate human and environmental risks *Critical Reviews in Environmental Science and Technology* **45** 1409–68
- Pastor A V, Ludwig F, Biemans H, Hoff H and Kabat P 2014 Accounting for environmental flow requirements in global water assessments *Hydrol. Earth Syst. Sci.* **18** 5041–59
- Pesaresi M, Ehrlich D, Kemper T, Siragusa A, Florczyk A, Freire S and Corbane C 2017 *Atlas of the Human Planet 2017. Global Exposure to Natural Hazards. EUR 28556 EN* (Joint Research Centre) p 92
- Poff N L and Zimmerman J K H 2010 Ecological responses to altered flow regimes: A literature review to inform the science and management of environmental flows *Freshwater Biology* **55** 194–205
- Reuter H I, Nelson A and Jarvis A 2007 An evaluation of void-filling interpolation methods for SRTM data *Int. J. Geogr. Inf. Sci.* **21** 983–1008
- Riahi K et al 2017 The Shared Socioeconomic Pathways and their energy, land use, and greenhouse gas emissions implications: An overview *Global Environ. Change* **42** 153–68
- Rosenzweig C, Solecki W, Hammer S A and Mehrotra S 2010 Cities lead the way in climate-change action *Nature* **467** 909–11
- Sharifi A 2021 Co-benefits and synergies between urban climate change mitigation and adaptation measures: A literature review *Sci. Total Environ.* **750** 141642

- Simpkins G 2018 Running dry *Nat. Clim. Change* **8** 369
- Simpson N P, Simpson K J, Shearing C D and Cirolia L R 2019 Municipal finance and resilience lessons for urban infrastructure management: a case study from the Cape Town drought *International Journal of Urban Sustainable Development* **11** 257–76
- Singh C, Jain G, Sukhwani V and Shaw R 2021 Losses and damages associated with slow-onset events: Urban drought and water insecurity in Asia *Current Opinion in Environmental Sustainability* **50** 72–86
- Sperna Weiland F C, Van Beek L P H, Kwadijk J C J and Bierkens M F P 2010 The ability of a GCM-forced hydrological model to reproduce global discharge variability *Hydrol. Earth Syst. Sci.* **14** 1595–621
- Stahl K et al 2016 Impacts of European drought events: Insights from an international database of text-based reports *Natural Hazards and Earth System Sciences* **16** 801–19
- Stanke C, Kerac M, Prudhomme C, Medlock J and Murray V 2013 Health effects of drought: A systematic review of the evidence *PLoS Currents* **5**
- Straatsma M et al 2020 Global to regional scale evaluation of adaptation measures to reduce the future water gap *Environ. Modell. Softw.* **124** 104578
- Sundberg R and Melander E 2013 Introducing the UCDP georeferenced event dataset *Journal of Peace Research* **50** 523–32
- Sutanudjaja E H et al 2018 PCR-GLOBWB 2: A 5 arcmin global hydrological and water resources model *Geoscientific Model Development* **11** 2429–53
- Tangdamrongsub N, Steele-Dunne S C, Gunter B C, Ditmar P G, Sutanudjaja E H, Sun Y, Xia T and Wang Z 2017 Improving estimates of water resources in a semi-arid region by assimilating GRACE data into the PCR-GLOBWB hydrological model *Hydrol. Earth Syst. Sci.* **21** 2053–74
- UN-DESA 2019 *World Urbanization Prospects: The 2018 Revision* (New York: United Nations: United Nations, Department of Economic and Social Affairs) p 126
- UNDRR 2019 *GAR Global Assessment Report on Disaster Risk Reduction* (United Nations Office for Disaster Risk Reduction (UNDRR))
- UNDRR 2021 *Special Report on Drought 2021* (Geneva, Switzerland: United Nations Office for Disaster Risk Reduction)
- UN-Habitat 2018 Tracking progress towards inclusive, safe, resilient and sustainable cities and human settlements *Tracking Progress Towards Inclusive, Safe, Resilient and Sustainable Cities and Human Settlements* (United Nations) (<https://doi.org/10.18356/36ff830e-en>)
- United Nations (Habitat III) 2017 *New Urban Agenda United Nations Conference on Housing and Sustainable Urban Development (Habitat III)* (Quito, Ecuador, 20 October 2016) www.habitat3.org
- Van Huijstee J, Van Bommel B and Van Rijn F 2018 *Towards an Urban Preview: Modelling future urban growth with 2UP* (PBL Netherlands Environmental Assessment Agency)
- Van Lanen H A J et al 2017 Climatological risk: droughts *Science for Disaster Risk Management 2017: Knowing better and losing less* ed K Poljanšek, M Marin Ferrer, T De Groeve and I Clark (Luxembourg: Publications Office of the European Union) pp 244–65
- Van Loon A F 2015 Hydrological drought explained *WIREs Water* **2** 359–92
- Van Loon A F et al 2016 Drought in the Anthropocene *Nat. Geosci.* **9** 89–91
- Van Loon A F and Van Lanen H A J 2012 A process-based typology of hydrological drought *Hydrol. Earth Syst. Sci.* **16** 1915–46
- Van Loon A F and Van Lanen H A J 2013 Making the distinction between water scarcity and drought using an observation-modeling framework *Water Resour. Res.* **49** 1483–502
- van Vliet M T H, Jones E R, Flörke M, Franssen W H P, Hanasaki N, Wada Y and Yearsley J R 2021 Global water scarcity including surface water quality and expansions of clean water technologies *Environ. Res. Lett.* **16** 12024020
- Von Uexkull N, Croicu M, Fjelde H and Buhaug H 2016 Civil conflict sensitivity to growing-season drought *PNAS* **113** 12391–6
- Wada Y et al 2016 Modeling global water use for the 21st century: The Water Futures and Solutions (WFaS) initiative and its approaches *Geoscientific Model Development* **9** 175–222
- Wang L, Gao J, Zou C, Wang Y and Lin N 2017 Water scarcity in Beijing and countermeasures to solve the problem at river basins scale *IOP Conf. Ser.: Earth Environ. Sci.* **94** 012132
- Ward P J et al 2020 Review article: Natural hazard risk assessments at the global scale *Natural Hazards and Earth System Sciences* **20** 1069–96
- Ward P J, Strzepek K M, Pauw W P, Brander L M, Hughes G A and Aerts J C J H 2010 Partial costs of global climate change adaptation for the supply of raw industrial and municipal water: A methodology and application *Environ. Res. Lett.* **5**
- Weedon G P, Balsamo G, Bellouin N, Gomes S, Best M J and Viterbo P 2014 Data methodology applied to ERA-Interim reanalysis data *Water Resour. Res.* **50** 7505–14
- Wilcoxon F 1945 Individual comparisons by ranking methods *Biometrics Bulletin* **1** 80–3
- Wilts R, Latka C and Britz W 2021 Who is most vulnerable to climate change induced yield changes? A dynamic long run household analysis in lower income countries *Climate Risk Management* **33** 100330
- Winsemius H C, Jongman B, Veldkamp T I E, Hallegatte S, Bangalore M and Ward P J 2018 Disaster risk, climate change, and poverty: assessing the global exposure of poor people to floods and droughts *Environment and Development Economics* **23** 328–48
- WMO & GWP 2016 *Handbook of Drought Indicators and Indices* ed M Svoboda and B A Fuchs (Integrated Drought Management Programme (IDMP)) (*Integrated Drought Management Tools and Guidelines Series 2*) (<https://doi.org/10.1201/9781315265551-12>)
- World Bank 2022 Poverty and Inequality Platform (version 20220909_2017_01_02_PROD) [data set]. World Bank <https://pip.worldbank.org/home>
- World Health Organisation & UNICEF 2021 Guidance note to facilitate country consultation on JMP estimates of WASH in health care facilities (<https://washdata.org/sites/default/files/2021-12/jmp-2021-winhcf-country-consultation.pdf#:~:text=The%20WHO%20and%20UNICEF%20joint%20monitoring%20programme%20for%20water%20supply%2C,progress%20on%20drinking%20water%20and%20sanitation%20and%20hygiene%20and%20WASH%29>)
- Yin Y, Zhang X, Lin D, Yu H, Wang J and Shi P 2014 GEPIIC-V-R model: A GIS-based tool for regional crop drought risk assessment *Agric. Water Manage.* **144** 107–19
- Zaag P V D and Savenije H H G 2006 *Water as an economic good: The value of pricing and the failure of markets* (UNESCO-IHE Institute for Water Education)
- Zaherpour J et al 2018 Worldwide evaluation of mean and extreme runoff from six global-scale hydrological models that account for human impacts *Environ. Res. Lett.* **13**
- Zhang X et al 2019 Urban drought challenge to 2030 sustainable development goals *Sci. Total Environ.* **693** 133536
- Zhou Y and Tol R S J 2005 Evaluating the costs of desalination and water transport *Water Resour. Res.* **41** 1–10
- Ziervogel G 2019 *Unpacking the Cape Town drought: Lessons learned* pp 1–26 African Centre for Cities